Available online at www.sciencedirect.com

ScienceDirect

Procedia CIRP 125 (2024) 213–218

www.elsevier.com/locate/procedia

CIRP BioM 2024

Robotic Bending of Craniomaxillofacial Fixation Plates

Brian Thurston[a], Javier Vazquez-Armendariz[a,b,c], Luis H. Olivas-Alanis[a], David Dean[a,d], Glenn Daehn[a]

[a] Department of Materials Science and Engineering, The Ohio State University, 140 W 19th Ave, Columbus, OH. 43212, United States [b] Tecnologico de Monterrey, School of Engineering and Sciences, 2501 Eugenio Garza Sada Av. Monterrey, N. L. 64849,
[c] Laboratorio Nacional de Manufactura Aditiva y Digital (MADIT), 100 Alianza Norte Av. Apodaca, N. L. 66629, Mexico
[d] Department of Plastic and Reconstructive Surgery, The Ohio State University, 915 Olentangy River Rd.Columbus, OH, 43212, United States

* Corresponding author. Tel.: 614-323-1165 E-mail address: Thurston.56@osu.edu

Abstract

While personalized, 3D printed, craniomaxillofacial (CMF) fixation plates are available from several vendors, given the short time window for reconstructive surgery in either advanced stage cancer resection or trauma, fixation plates are most often manually bent by eye. A surgeon's manual bending of fixation plates may significantly delay these time-sensitive procedures as well as introduce work hardening damage to the plate due to repetitive bending at one or more locations. Unfortunately, revision surgery can follow work hardening-induced fatigue failure, stress-shielding-induced bone loss, or stress concentration-induced fixation device failure. Our group has developed a desktop automated fixation plate bending unit for the robotic bending of CMF fixation plates. Our automated plate bending device consists of a pair of modular jaws that precisely hold a fixation plate and iteratively bend/twist it based on geometric data imported from a plate bending plan developed using 3D patient data and a VSP (Virtual Surgical Planning) environment. Our prototype plate bender offers accurate plate bending in a time frame that is much reduced versus traditional manual plate bending. The design details, and performance of this device are documented in this study.

Keywords: Biomanufacturing; Robotics, Craniomaxillofacial, Fixation Plates, PET-FAB (Physical Exploration and Training – Factor Automation Box).

1. Introduction

Craniomaxillofacial (CMF) deformities due to malformation, trauma, or tumor resection may be treated with surgical reconstruction and possibly bone grafts. Cut segments of bone that are newly mobile require at least one metallic fixation plate while they are healing in place. These fixation plates are most often formed from medical grade Titanium Ti6Al-4V. These fixation systems are offered in a large variety of geometries and are used to bring together bony disunions, or to offer stability to a reconstructive bone graft [1]. In addition, to shape and thickness, fixation plate selection will depend on the reconstructed area's load-bearing requirements [2]. Some fixation plates are a linear series of equidistant screw-hole bosses connected by small bridges. The screw holes permit easy fixation of the plate to bony surfaces, while the bridges between the screw holes offer a convenient location for customizing the fixation device by plastic bending and twisting.

Since most of the off-the-shelf commercially available fixation plates are not personalized, the physician will try to fit them to the curving bony surface by repeatedly bending until a good fit is achieved during open surgery [2]. Efforts to reduce the surgery time have focused on the use of anatomical 3Dprinted models to conduct plate bending in a pre-surgical environment [3]. Having a plate flush to the bone, without any bone-plate interface gaps, will increase the stability of the locking connections (i.e., threaded screw eyelets and screw heads locked tightly against the bone) [4]. However, even a well-fitting plate may fail in situ if the physician work-hardens the metal with extensive and repeated bending of the plate in an effort to achieve a good fit [5].

Promising new CMF therapies consider the use of Computer-Aided Design (CAD) tools to enable the creation of Virtual Surgical Planning (VSP) environments where a patient's specific anatomical model can be obtained and visualized in 3D [6]. Furthermore, the fixation plate can be contoured to the bony surface, by planning its location and shape. With this information, the bending required can be

10.1016/j.procir.2024.08.037

easily computed. Even though a VSP environment can enable the production of patient-specific fixation plates via Additive Manufacturing (AM) technologies, such as Powder Bed Fusion (PBF), not all procedures that would benefit from them are covered by insurance. Moreover, AM build sessions are usually costly, time-consuming, and parts produced may require postprocessing to get rid of partially-sintered attached particles, since their presence may cause an inflammatory response in surrounding tissues, if released [7][8].

1.1. Motivation for this work

Despite the progressive learning of surgeons on the optimal ways to bend fixation plates to achieve the desired shape, it is difficult to impossible to conduct manual bending as efficiently as a pre-planned robotic work path. Hence, we are working on a robotic system capable of achieving this work with the least deformation possible. Similarly, there are several systems capable of shaping wires for orthodontic applications [9] or titanium meshes. Nevertheless, to the authors' best knowledge, there is just one work on the robotic bending of fixation plates for oral and maxillofacial surgery. In that paper Zhang et al., designed and fabricated a three-axis forming robot that numerically controls the bending of medical titanium plates to improve accuracy and efficiency compared to the standard manual bending process. However, further experimentation was needed to incorporate VSP tools to provide the appropriate bending angles to accurately fit a human mandible model [10].

Recently, our research group showed early-stage testing of a workflow that embraces the benefits of Metamorphic Manufacturing [11] to design and personalize medical device´s shape simultaneously with its function by means of Hybrid Autonomous Manufacturing modalities [12]. Our "manufacture for design" approach aims to produce devices at the Point-ofCare, such as the fixation plates to be showcased in this work for CMF applications, with optimal shape and mechanical performance based on biomechanical data derived from VSP [13]. This same approach can be extended to other relevant applications, such as the modeling of optimized function, design, and performance of load-bearing percutaneous implants [14].

Therefore, this work focuses on the evolution of a crucial part of that workflow. (stage 3 – 4: process engineering and manufacturing [12]), which has been improved by the development of a desktop sized automated fixation plate bending device. In the next sections the design and fabrication of our plate bending unit will be described. Validation of the bending capabilities will be discussed with different VSPdesigned titanium test plates designed to fit a human skull that we simulate virtually and have 3D printed to manually validate the fit of rendered fixation plates. The resulting bend accuracy will also be demonstrated, and future directions will be discussed.

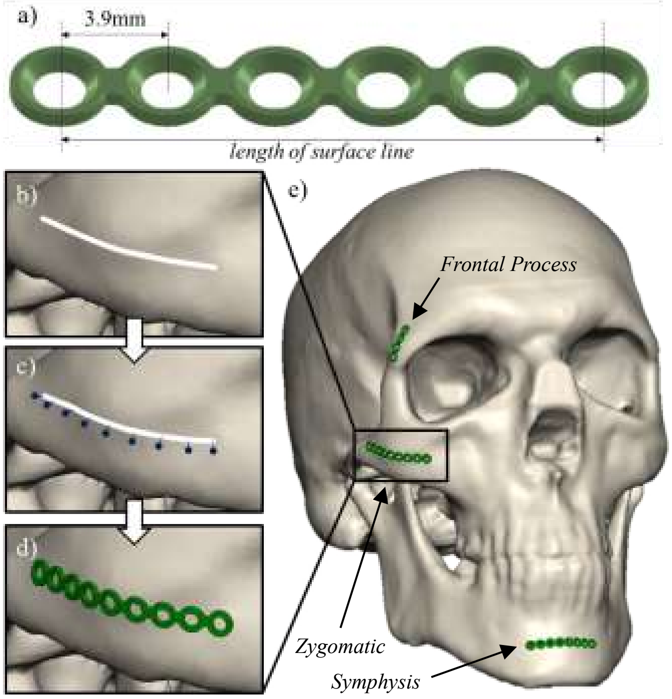

Fig. 1. Workflow for VSP design of tes t plates. Three example plates are shown and are labelled according to the anatomy they cover: Frontal Process, Zygomatic, and Symphysis. a). Our CMF plate design, which is based off existing commercially available plate designs. b). Fitting of plate to skull anatomy. c). Spacing of screw hole intervals. d). Final plate profile to obtain bending angles. e) Placement of VSP designed test plates on a skull model.

2. Materials and Methods

2.1. Virtual Surgical Planning (VSP)

For this VSP work we used a human skull model derived from the Visible Human Project [15]. However, clinical VSP would involve the collection of a similar set of Computerized Tomography (CT) images of the patient´s head. An anatomical surface model is created by distinguishing the bone from other surrounding tissues (i.e., muscle, fat, skin, brain, etc.), based on density differences (i.e., thresholding based on a user-selected grayscale range) with the potential for manual correction when non-skeletal objects are obtained, or skeletal objects are insufficiently obtained.

Once an accurate anatomical model of the bone surfaces in need of fixation are acquired VSP work for CMF plate placement can begin. Using the skull model from the Visible Human Project, the location, shape, and length of three different CMF plates were planned in Geomagic Freeform software (3D systems, Rock Hill, SC), as seen in Fig. 1. These three test plates will be referred to as the Frontal Process, Zygomatic Arch, and Mental Symphysis plates. For this application, a 0.5 mm thick CMF plate, with a distance between screw hole centers of 3.9 mm and a hole diameter of 1.9 mm was used Fig. 1(a). At locations of interest a line was drawn and fitted to the skull's surface curvature where a disunion (or bone graft) may be located Fig. 1(b). The length of this surface line corresponds to the distance between the center of the first and the last screw holes in the final fixation plate design. Next, the

could be placed (4 for the Frontal Process, 9 for the Zygomatic line was divided such that the intended number of screws Arch, and 8 for the Mental Symphysis plates), marks were positioned to indicate the location of each screw, Fig. 1(c). Finally, a CMF plate model was generated according to the contour of the line, Fig. 1(d). Unit vectors corresponding to the direction of screw placement were collected from the CMF plate design, these unit vectors were similar, but not identical to the surface normal lines shown in Fig. 1(c). Euler angles for bending and twisting between each screw hole were calculated. These angles represent the necessary bending/twisting of a CMF plate that a surgeon or robotic system would need to apply to achieve proper placement against the target bone surface.

2.2. The automated plate bending system

Robotic bending of fixation plates appears to have been first described by Zhang et al. [10]. Looking at the work of Zhang et al., we had the same concern that they had when considering the use of six axis robots. We wished to progress from one end of the plate to the other and effect the simplest bend routine so as to have the most space to effect a bend and twist operation, to avoid risking work-hardening from revisiting a site, and to produce the bent plate as quickly as possible. In regards to the first problem to solve, avoiding parts hitting each other in the small bending operation workspace, we chose a simplified robotic plate bending system composed of a 2 axis gimbal mechanism and a single linear actuator for plate bending and indexing. Within that space we attached two pairs of pneumatically actuated jaws, one to each gimbal, for grasping two adjacent screw eyelets on the CMF plate. This plate bender design, shown in Fig. 2, is capable of applying twists and out of plane bends to the connecting geometry between screw holes on a fixation plate. It is also capable of indexing along the length of straight fixation plates.

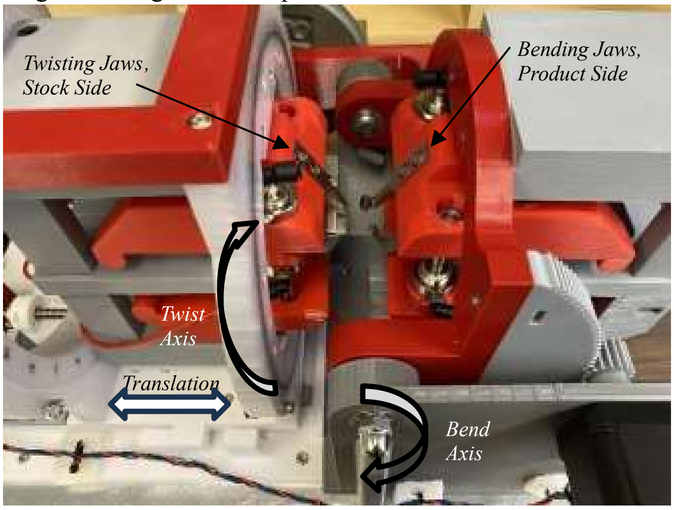

Fig. 2. The prototype automatic plate bender, known internally as the "Bendy Bot".

In addition to the gimbal parts not hitting each other, the jaw tips of the automatic plate bender were specifically designed to prevent intersection (i.e., collision) with one another during bending and twisting. The jaw geometry permits ±30° twisting

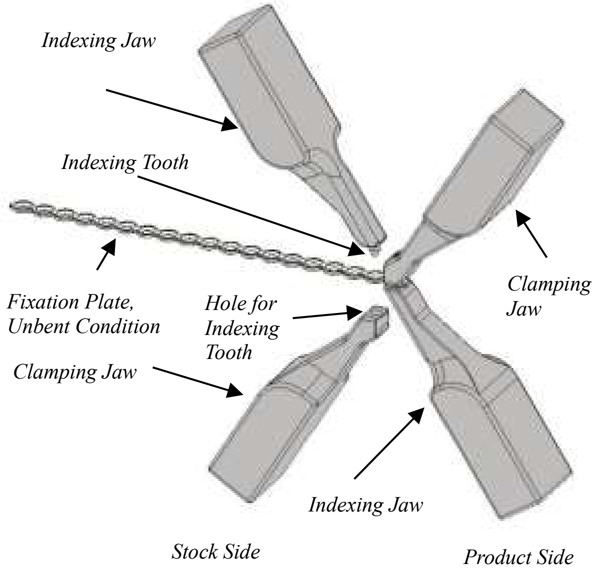

Fig. 3. The jaw design used for bending and twisting the CMF plates.

and +30° to -15° out of plane bending of the fixation plate, and any combination of bending and twisting within those ranges. An overview of the jaw geometry is shown in Fig. 3 and Fig. 4, where a bend in the positive (+) direction is clockwise.

In Fig. 2&3 two pairs of jaws are shown, labelled the stock side and the product side jaws. An unbent fixation plate enters from the stock side and leaves through the product side during bending. There are two types of jaws on each gimbal, an indexing jaw and a clamping jaw. The indexing jaw possesses an indexing feature, a tooth in this case, which is used to locate the screw holes of the fixation plate. Pressure is applied by the clamping jaw, which includes a hole to accept any amount of the indexing tooth which protrudes beyond the thickness of the fixation plate. The presence of this hole necessitated thickening of the clamping jaw's tip. This thickened tip, coupled with the need to open only the stock side jaws when indexing, is what produces the asymmetrical +30° to -15° out of plane bending limitation as the thickened section of the clamping jaw can interfere with opening of the stock side jaws beyond a -15° bend. The indexing and clamping jaws are inverted on the product side in Fig. 3 because otherwise the bending limit in the negative direction would be even less than -15°.

In Fig. 4 the general sequence for bending and indexing of a CMF plate is shown. Fig. 4(a) depicts the position of the jaws following a 30° out of plane bend. In Fig. 4(b) the stock side jaws (left) are shown in the open position. Notice that in Fig. 4(a&b) the jaws do not conflict during bending and opening. As mentioned, the need to eliminate jaw conflicts was a major driver of the design of the automated plate bender. In Fig. 4(b) the stock side jaws are also translated to the left by the centerto-center distance of the plate's screw holes, leaving the stock side indexing tooth directly over the next eyelet to the left of the stock side jaw starting position in Fig. 4(a). In Fig. 4(c) the stock side indexing jaw is moved down into contact with the fixation plate and its indexing tooth is inserted into the eyelet. Simultaneously, pressure is applied by the stock side clamping jaw, thereby reestablishing a firm grasp of the plate by the stock side jaws. In Fig. 4(d&e) the product side jaws (right) are released and rotated back to the origin. Additionally, in Fig. 4(e) the stock side jaws are shown translated back to the right by the center-to-center distance of the screw holes, this time leaving the indexing tooth of the product side jaws directly under the screw hole which the stock side jaws were clamped onto in Fig. 4(a). In Fig. 4(f) the product side jaws are shown in the closed position ready to make an additional bend or twist to the CMF plate. By this process a sequence of clockwise or counterclockwise bends may be applied to the plate between successive eyelet pairs. Because the plate is always held rigidly by one or both of the stock and product side jaws, the fixation plate will always have a known position determined by at least one indexing tooth. By the sequence of steps shown in Fig. 4 a CMF plate may be 'walked' from the stock side to the product side where each eyelet pair receives a specified bend or twist, resulting in a CMF fixation plate which matches the curvature of the target bone surface.

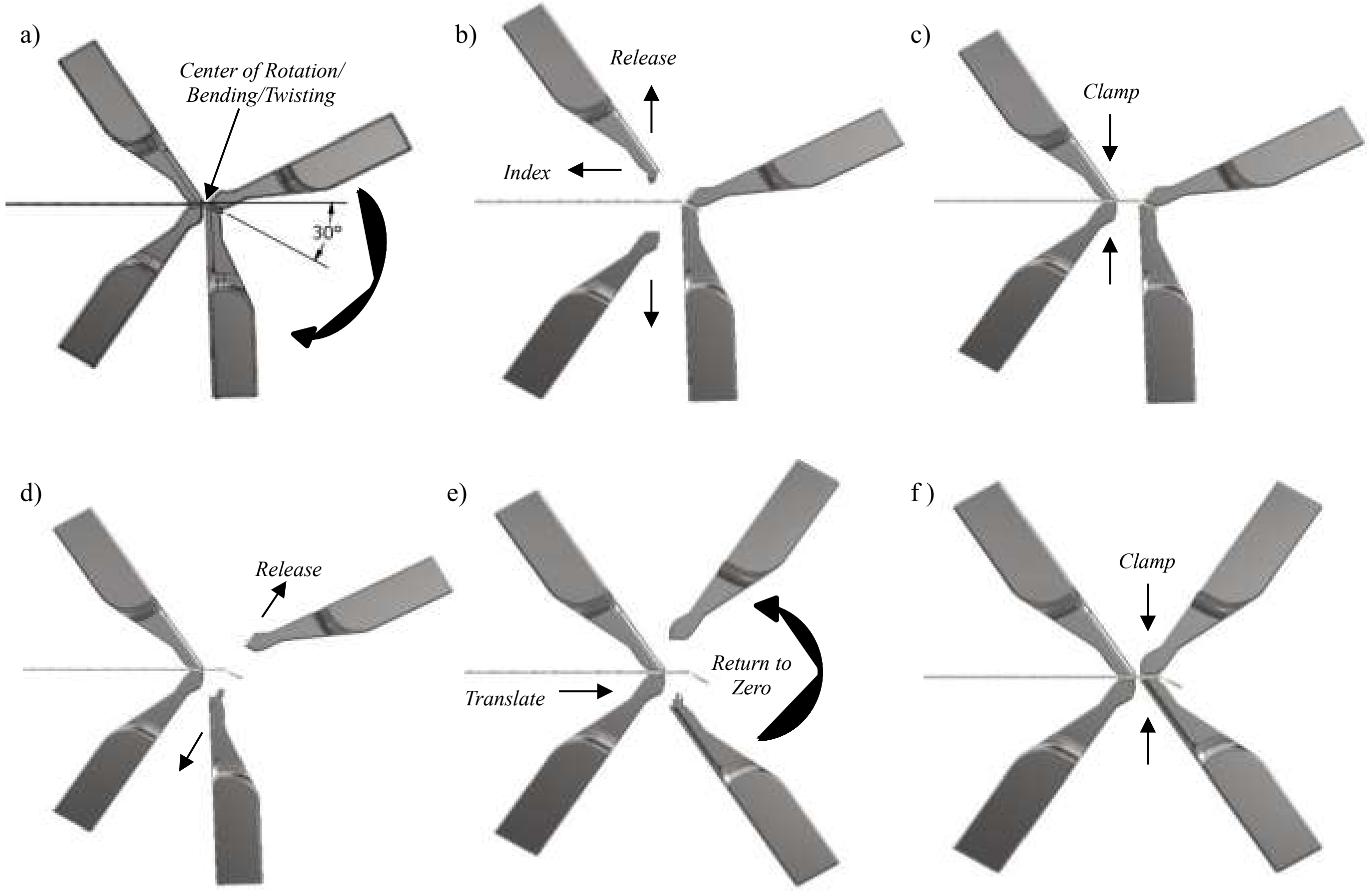

Fig. 4. The general sequence for indexing between screw holes on a fixation plate after applying a bend. At all times the CMF plate is held rigidly between at least one pair of jaws to keep its position fixed to a known location as it is indexed through the automatic plate bender.

2.3. Laser cutting of titanium CMF plates

Custom CMF plates were manufactured for this study to prepare for definitive testing with expensive surgical grade CMF plates. These locally manufactured plates are shown in Fig. 5. The design shown in Fig. 1(a) was used. We manufactured these plates by laser cutting with a Raycus brand 30-watt fiber laser engraver from 0.5 mm thick grade 2 titanium sheet. This grade 2 titanium had a yield strength of 275MPa. The laser was able to cut the 0.5 mm thick titanium sheet in 8 passes at a cutting speed of 100 mm/s. During these passes the laser deposited enough heat into the titanium to cause visible discoloration. This heat likely altered the material properties of the titanium alloy. Since these plates were intended only for use

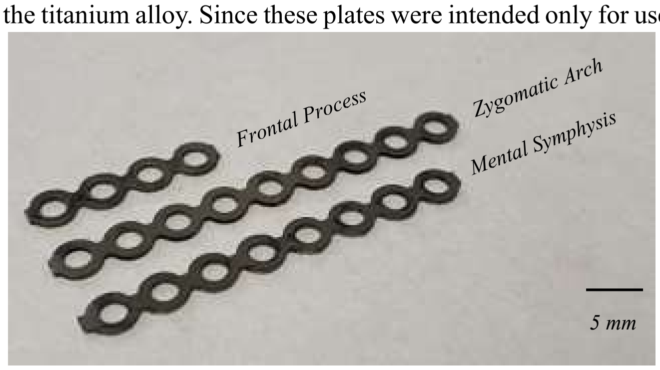

Fig. 5. The CMF fixation plates cut from grade 2 titanium.

in demonstrating the robotic bending process these material property changes were deemed acceptable. The final dimensions of the CMF plates that we made matched those of the plates shown in Fig. 1 within ±0.1 mm, however, the chamfer around the screw holes had to be omitted since the laser cutter was unable to cut this feature.

2.4. Springback calibration and Accuracy Assessment

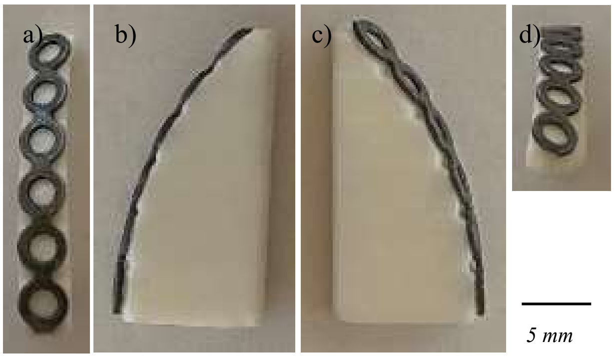

Fig. 6. Four viewing perspectives of a test CMF plate placed against a 3D printed test object showing good fit across the entire surface.

It was necessary to have some means of calibrating the automatic plate bender to compensate for springback of the titanium CMF fixation plates after bending. In practice calibration constants will be used to overbend and/or overtwist the CMF plates such that after springback they will have the appropriate bend/twist angle. The twisting and out of plane bending calibration constants were found by repeatedly bending/twisting sample laser cut CMF plates to a variety of angles (3°, 5°, 6°, and 9°) and then measuring the difference between the target angle and the actual angle of the bend. It was found that calibration constants of 5.5° for bending and 4.8° for twisting were acceptable over the range from 1° to 10°. Beyond 10° these compensation angles were less effective. Once the calibration constants were known, a test surface was 3D printed which would require a plate with five 9° out of plane bends and five 6° twists to match its surface. A six-hole laser cut CMF plate was successfully bent by the automatic plate bender, the result is shown in Fig. 6 from four different viewing perspectives.

Fig. 7. The skull model with the plates placed.

3. Results

Bending of the three fixation plate designs proceeded with only one manufacturing process concern, the cumulative bending of the Zygomatic Arch plate resulted in a conflict between the geometry of the bent plate and the structure of the automatic plate bender. This conflict required the Zygomatic Arch plate be shortened from 9 to 8 eyelets. After manual insertion of the stock plate, the automatic plate bender produced the Frontal Process plate in about 25 seconds. The Zygomatic Arch and Mental Symphysis plates required about 45 seconds to be completed by the automatic plate bender.

A 3D print of the skull model in Fig. 1 was produced with superficial holes placed at the intended locations of the fixation screws. This skull model can be seen with the test CMF plates attached in Fig. 7 and Fig. 8. In Fig. 8(b) the extra hole for the omitted 9th Zygomatic Arch screw hole is visible.

Close up views of the CMF plates at their intended installation sites are given in Fig. 8. The overall fit of the fixation plates was satisfactory for a first prototype plate bending system, however, for surgical application the quality of the fit should be improved. For the Frontal Process plate three of the four screw holes lied flush to the model surface,

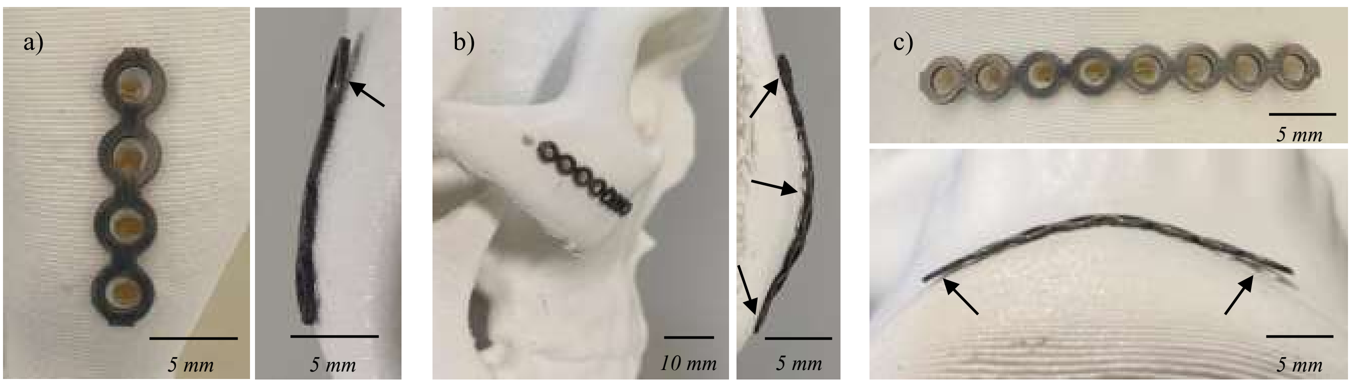

Fig. 8. Front and side views of the test fixation plates placed against a 3D printed skull. This 3D printed skull was modified with superficial holes at the intended screw placement points for the test CMF plates. The black arrows indicate areas of poor fit. a). Views of the Frontal Process plate. b). The Zygomatic Arch plate. The location of the intended 9th screw hole is visible on the 3D printed skull surface. c). The Mental Symphysis plate.

with the last screw hole being bent slightly away from the model. The Zygomatic Arch plate deviated from the target surface at the three locations indicated by the black arrows in Fig. 8(b). Four of the eight screw holes of the Zygomatic Arch plate were flush to the model surface. The Mental Symphysis plate was flush across its center, with deviations from the target model present at either end, as indicated in Fig. 8(c).

The errors in plate bending in Fig. 8 may arise from several sources. These include poor springback calibration for certain angles, especially the few bend angles beyond 10° required by the Zygomatic and Symphysis plates. Compounding errors arising from small deviations from the bend/twist target likely also had an effect. Occasional large bend errors at the stock side end of the plates have also been observed, this is likely related to the fact that the final stock side eyelet is not and cannot be indexed through the machine like all the other eyelets, see Fig 4. This issue may be addressed with a sacrificial eyelet.

4. Conclusion and Discussion

The initial instantiation of our robotic plate bending device performed well in our VSP design planning and fabrication tests. We identified further improvements that will be incorporated in the fixation plate bender design and bending process. These include closed loop feedback, angular measurement, and a more rigid construction of the plate bender. Overall, the results of our validation tests are promising. We have confirmed that a linear, progressive approach to bending appears to provide results that have clinical applicability. We therefore have not taken the approach of Zhang et al. [10] and those who have attempted wire-bending for clinical applications. Our VSP process of fixation plate bending which incorporates principles of Metamorphic Manufacturing shows promise for clinical point of care manufacturing of CMF plates. Our process could lead to a reduction in surgery times and an increase in surgical reconstruction quality. Rapidly and accurately manufactured CMF plates which do not require iterative bending by the surgeon may be less prone to fatigue cracking and may also reduce the incidence of disunion.

Acknowledgments

This project received support from the Department of Materials Science and Engineering at The Ohio State University. The authors wish to acknowledge a President's Research Excellence (PRE) Catalyst grant, titled "Hybrid Autonomous Point-of-Care Manufacturing", from The Ohio State University and a United States National Science Foundation Engineering Research Center grant (EEC-2133630), titled "Hybrid Autonomous Manufacturing: Moving from Evolution to Revolution" (https://hammer.osu.edu).

Author Contributions

Conceptualization, G.D., D.D., B.T., J.V.A., L.H.O.A; methodology, B.T., and J.V.A.; software, B.T., and L.H.O.A; validation and data curation, B.T; resources, G.D., and D.D.; writing—original draft preparation, B.T., J.V.A., and L.H.O.A; writing—review and editing, B.T., J.V.A., L.H.O.A and D.D.; project administration, D.D., and G.D.; funding acquisition, D.D., and G.D.

Patents

Portions of this work are subject to pending patent applications in which B.T., J.V.A., D.D., and G.D. are inventors.

Conflicts of Interest

Outside of the interest of the four authors in several pending patent applications, see "Patents", the authors declare no conflict of interest.

References

[1] B. T. Goh, S. Lee, H. Tideman, and P. J. W. Stoelinga, "Mandibular reconstruction in adults: a review," Int J Oral Maxillofac Surg, vol. 37, no. 7, pp. 597–605, Jul. 2008, doi: 10.1016/j.ijom.2008.03.002.

[2] I. Campioni, I. Cacciotti, and N. Gupta, " Additive manufacturing of reconstruction devices for maxillofacial surgery: design and accuracy assessment of a mandibular plate prototype," Annali Dell Istituto Superiore Di Sanita, vol. 50, no. 2, pp. 136–145, 2020.

[3] M. Azuma et al., "Mandibular reconstruction using plates prebent to fit rapid prototyping 3-dimensional printing models ameliorates contour deformity," Head Face Med, vol. 10, no. 1, p. 45, Dec. 2014, doi: 10.1186/1746-160X-10-45.

[4] P. Bujtár, J. Simonovics, K. Váradi, G. K. B. Sándor, and C. M. E. Avery, "The biomechanical aspects of reconstruction for segmental defects of the mandible: A finite element study to assess the optimisation of plate and screw factors," Journal of Cranio-Maxillofacial Surgery, vol. 42, no. 6, pp. 855–862, Sep. 2014, doi: 10.1016/j.jcms.2013.12.005.

[5] M. Martola, C. Lindqvist, H. Hänninen, and J. Al‐Sukhun, "Fracture of titanium plates used for mandibular reconstruction following ablative tumor surgery," J Biomed Mater Res B Appl Biomater, vol. 80B, no. 2, pp. 345–352, Feb. 2007, doi: 10.1002/jbm.b.30603.

[6] A. Alkhayer, J. Piffkó, C. Lippold, and E. Segatto, "Accuracy of virtual planning in orthognathic surgery: a systematic review," Head Face Med, vol. 16, no. 1, p. 34, Dec. 2020, doi: 10.1186/s13005-020-00250-2.

[7] M. H. Mobarak et al., "Recent advances of additive manufacturing in implant fabrication – A review," Applied Surface Science Advances, vol. 18, p. 100462, Dec. 2023, doi: 10.1016/j.apsadv.2023.100462.

[8] Chemical Polishing of Additively Manufactured, Porous, Nickel–Titanium Skeletal Fixation Plates https://www.liebertpub.com/doi/full/10.1089/3dp.2020.0209

[9] J. Jiang, Y. Zhang, C. Wei, T. He, and Y. Liu, "A Review on Robot in Prosthodontics and Orthodontics," Advances in Mechanical Engineering, vol. 7, no. 1, p. 198748, Jan. 2015, doi: 10.1155/2014/198748.

[10] J. Zhang, B. Shi, G. Feng, G. Zuo, and Y. Liang, "Design, Development and Control of a Forming Robot for an Internally Fixed Titanium Alloy Strip," Machines, vol. 10, no. 2, p. 68, Jan. 2022, doi: 10.3390/machines10020068.

[11] The Minerals, Metals & Materials Society (TMS), Metamorphic Manufacturing: Shaping the Future of On-Demand Components (Pittsburgh, PA: TMS, 2019). Electronic copies available at www.tms.org/metamorphicmanufacturing.

[12] Vazquez-Armendariz, J., Olivas-Alanis, L.H., Mahan, T. et al. Workflow for Robotic Point-of-Care Manufacturing of Personalized Maxillofacial Graft Fixation Hardware. Integr Mater Manuf Innov 12, 92–104 (2023). https://doi.org/10.1007/s40192-023-00298-3

[13] Dean, D. et al. Virtual Surgical Planning for Point-of-Care Manufacturing CIRP Biomanufacturing 2024. "In revision".

[14] Olivas-Alanis, L. H. et al. Introduction of Finite Element Analysis to Virtual Surgical Planning for the Design of Stiffness-Matched, Personalized Load-Bearing Percutaneous Implants. CIRP Biomanufacturing 2024. "In revision"

[15] National Institutes of Health. (n.d.). The National Library of Medicine's Visible Human Project. U.S. National Library of Medicine. https://www.nlm.nih.gov/research/visible/visible_human.html